Letter

Ferromagnetic ordering of magnetic impurities mediated by supercurrents in the presence of spin-orbit coupling

Yao Lu [1,*] I. V. Tokatly [2,3,4,†] and F. Sebastian Bergeret [1,4,‡]

[1] *Centro de Física de Materiales (CFM-MPC), Centro Mixto CSIC-UPV/EHU, E-20018 San Sebastián, Spain*
[2] *Nano-Bio Spectroscopy Group, Departamento de Polímeros y Materiales Avanzados, Universidad del País Vasco, 20018 Donostia–San Sebastián, Basque Country, Spain*
[3] *IKERBASQUE, Basque Foundation for Science, 48009 Bilbao, Basque Country, Spain*
[4] *Donostia International Physics Center (DIPC), 20018 Donostia–San Sebastián, Spain*

(Received 25 July 2023; revised 29 September 2023; accepted 3 November 2023; published 15 November 2023)

We investigate the behavior of magnetic impurities placed on the surface of superconductor thin films with spin-orbit coupling. Our study reveals long-range interactions between the impurities, which decay according to a power law, mediated by the interplay between the superfluid response described by the London equations and the anomalous supercurrents due to magnetoelectric effects. Importantly, these interactions possess a ferromagnetic component when considering the influence of the electromagnetic field, leading to the parallel alignment of the magnetic moments in the case of two impurities. In a Bravais lattice of magnetic impurities, superconductivity facilitates the establishment of ferromagnetic order within specific parameter ranges. These findings challenge the conventional understanding that ferromagnetism and superconductivity are mutually exclusive phenomena. Our theoretical framework provides a plausible explanation for the recently observed remanent flux and transport signature of ferromagnetism in iron-based superconductors, particularly Fe(Se,Te).

DOI: 10.1103/PhysRevB.108.L180506

Introduction. Ferromagnetic ordering is often seen as incompatible with conventional superconductivity due to the presence of an effective exchange field in ferromagnets. This exchange field has the effect of breaking up Cooper pairs, which are composed of electrons in a singlet state [1]. The coexistence of these two orders, however, does exist in hybrid superconductor/ferromagnet (S/F) structures [2,3]. In these structures, the proximity effect plays a crucial role in enabling the coexistence of superconductivity and ferromagnetism. Singlet pairs can be transformed into triplet pairs through the exchange field of the F region. As a result, a local magnetic moment is produced, extending over distances of the order of superconducting coherence length ξ_s. This phenomenon is referred to as the magnetic or inverse proximity effect [4,5]. The generated magnetic moment is oriented in the opposite direction to the magnetization of the ferromagnetic region. In the case of a small ferromagnetic island, this results in the screening of its magnetic moment [6]. If a second ferromagnetic region (F region) is positioned at a distance smaller than ξ_s from the first ferromagnet, the energetically favorable arrangement is an antiparallel orientation of the magnetizations of the two F regions.

The antiparallel alignment serves as the basis for the FSF superconducting spin valve [7–10]. The studies on FSF structures with conventional superconductors indicate an antiferromagnetic coupling between the magnets, mediated by the inverse proximity effect. This coupling strength decreases exponentially with the distance between the ferromagnetic regions.

This situation changes in thin superconducting films with spin-orbit coupling (SOC). The combination of the exchange field generated by a magnetic impurity (m_1 in Fig. 1) and the SOC results in the spontaneous generation of anomalous currents through the spin-galvanic effect. In the case of a Rashba SOC they flow perpendicular to the magnetization (green arrows in Fig. 1) [11,12]. These anomalous currents are spatially localized [13] over the coherence length from the impurity. Charge conservation implies the emergence of a phase gradient, ensuring $\nabla \cdot \boldsymbol{j} = 0$ and the appearance of circulating currents [14] (black arrows in Fig. 1).

If we assume that a magnetic moment $\boldsymbol{m}_1$ points in the positive x direction (Fig. 1), then it generates a nonlocal circular supercurrent which flows in the negative y direction at the position of the magnetic impurity $\boldsymbol{m}_2$ and to the positive y direction at the position of $\boldsymbol{m}_3$. The orientations of $\boldsymbol{m}_{2,3}$ are determined by minimization of the free energy: To reduce the kinetic energy of the superflow they will generate anomalous currents that suppress the currents induced by $\boldsymbol{m}_1$. Consequently, $\boldsymbol{m}_2$ will point in the positive x direction and $\boldsymbol{m}_3$ to the negative x direction. In other words, the supercurrent-mediated magnetic interaction is ferromagnetic between $\boldsymbol{m}_1$ and $\boldsymbol{m}_2$ while it is antiferromagnetic for $\boldsymbol{m}_1$ and $\boldsymbol{m}_3$. Thus, in general, for two magnetic impurities, $\boldsymbol{m}_1$ and $\boldsymbol{m}_2$ the magnetic interaction will have the form

$$F_I = J_\perp \hat{\boldsymbol{m}}_{1\perp}\hat{\boldsymbol{m}}_{2\perp} - J_\parallel \hat{\boldsymbol{m}}_{1\parallel}\hat{\boldsymbol{m}}_{2\parallel}\ , \tag{1}$$

where $\hat{\boldsymbol{m}}$ is the unit vector in the direction of $\boldsymbol{m}$. $\perp$ ($\parallel$) denotes the component in the direction perpendicular (parallel) to $\boldsymbol{r} = \boldsymbol{r}_1 - \boldsymbol{r}_2$, and both $J\perp$ and $J_\parallel$ are positive.

*yao.lu@ehu.eus
†ilya.tokatly@ehu.es
‡fs.bergeret@csic.es

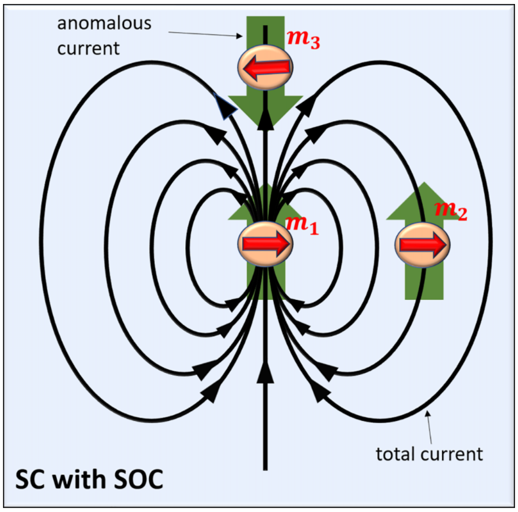

FIG. 1. Schematic picture of magnetic impurities on top of a superconductor thin film with spin-orbit coupling. The red arrows represent the magnetization of the impurities. The green arrows are the exchange field-induced localized anomalous currents. The black loop represents the total current induced by the exchange field, phase gradient, and electromagnetic field.

Previous studies on Rashba superconductors [14,15], specifically regarding the current distribution around a magnetic impurity and the induced magnetic interaction, have obtained an interaction resembling the two-dimensional (2D) dipole-dipole interaction (DDI) form with $J_\perp = J_\parallel$, which does not result in either a ferromagnetic or an antiferromagnetic ground state for two impurities [16]. However, those studies have neglected the influence of the electromagnetic (EM) field. On the other hand, we know from Pearl's seminal work [17] that the EM field plays a crucial role in determining the current distribution in conventional superconducting thin films. This leads to the natural question of the effect of the EM field on the magnetic coupling between impurities in a superconductor with spin-orbit coupling (SOC).

In this Letter, we present a theory elucidating the impact of the electromagnetic field on the magnetic coupling between impurities. We predict a ferromagnetic coupling in superconducting systems exhibiting magnetoelectric effects related to SOC, independently of the microscopic details [18]. We demonstrate that a combination of these effects and the superfluid response of the condensate, via the London equation, alters drastically the spatial dependence of the couplings $J_{\perp(\parallel)}$. We establish that the supercurrent-mediated magnetic interaction exhibits the form of a DDI that is generated by the so-called Keldysh potential [19,20], and interpolates between the 2D and 3D DDI. It can also be viewed as a 2D DDI combined with a ferromagnetic interaction, leading to a ferromagnetic ground state for two impurities.

Furthermore, we emphasize the crucial role of the EM field in a 2D impurity lattice. Without taking into account the EM field, the interaction energy density becomes unphysically divergent as the system size approaches infinity. However, when the EM field is included, the energy density converges in the limit of large system size.

In the remainder of this Letter, we provide a detailed derivation of these results and discuss recent experimental results suggesting a superconducting-induced ferromagnetic order of impurities in Fe(SeTe) [21], and propose other superconductors to verify our findings.

Theory. We consider magnetic impurities on top of a two-dimensional superconducting system, which can, for example, be a thin film on a substrate or superconductivity induced at the surface of a topological insulator. In these systems, the inversion symmetry is broken because of the presence of the intrinsic polar vector—the normal $\hat{z}$ to the transport plane. Additionally, the exchange field induced by the impurity's magnetic moment $\boldsymbol{m}$ locally breaks the time-reversal symmetry. In the presence of SOC, the breaking of these two symmetries implies the existence of a spontaneous current $\boldsymbol{j}_{\rm an}(\boldsymbol{r})$, known as anomalous current. This current is localized around the magnetic defect on the scale of the coherence length. The direction of the net anomalous current $\boldsymbol{J}_{\rm an} = \Gamma\hat{\boldsymbol{m}} \times \hat{z}$ is uniquely fixed by the symmetry [22,23], while its amplitude, parametrized by the coefficient Γ, is determined by the microscopic details of the underlying superconductor. To illustrate this point, in the Supplemental Material (SM) (Sec. 1) [24] we calculate Γ in different regimes for Rashba and Dirac superconductors.

It is convenient to parametrize the anomalous current density induced by all magnetic impurities in terms of an effective "background" vector potential $\boldsymbol{a}(\boldsymbol{r})$ using the London equation $\boldsymbol{j}_{\rm an}(\boldsymbol{r}) = -e^2 D\boldsymbol{a}(\boldsymbol{r})$, where D is the superfluid weight and e is the electron charge. The change of the free energy due to the supercurrent then reads

$$F = \int d^3\boldsymbol{r}\frac{1}{8}D[\nabla\phi - 2e\boldsymbol{A} - 2e\boldsymbol{a}]^2\delta(z) + \frac{1}{2\mu_0}\boldsymbol{B}^2, \tag{2}$$

where $\boldsymbol{A}$ is the electromagnetic vector potential, $\boldsymbol{B} = \nabla\times\boldsymbol{A}$ is the corresponding magnetic field, μ_0 is the magnetic constant, and we assume the superconductor film located at $z = 0$. The first term in Eq. (2) is the free energy of the superconductor $F_{\rm SC}$, attributed to the superflow. It reflects the superconducting response to the vector potential, and the existence of the anomalous current. The second term $\sim\boldsymbol{B}^2$ is the energy of magnetic field generated by the supercurrent. Note that $\boldsymbol{A}$ lives in three dimensions while $\nabla\phi$ and $\boldsymbol{a}$ are defined in the 2D superconductor. Taking the derivative of $F_{\rm SC}$ with respect to $-\boldsymbol{A}$, one obtains the 2D supercurrent flowing in the plane of the superconductor,

$$\boldsymbol{j} = \tfrac{1}{2}eD[\nabla\phi - 2e\boldsymbol{A} - 2e\boldsymbol{a}]\delta(z). \tag{3}$$

Minimizing the free energy with respect to ϕ gives the charge conservation $\nabla\cdot\boldsymbol{j} = \boldsymbol{0}$. In the following, we choose the Coulomb gauge $\nabla\cdot\boldsymbol{A} = \boldsymbol{0}$. This implies that the phase gradient cancels the longitudinal part $\boldsymbol{a}_l$ of the effective gauge field, which is written in the momentum $\boldsymbol{q}$ space as $\boldsymbol{q}\phi = 2e\boldsymbol{a}_l = 2e\boldsymbol{q}(\boldsymbol{q}\cdot\boldsymbol{a})/q^2$. The current of Eq. (3) is then fully determined by the transverse component $\boldsymbol{a}_t = \boldsymbol{a} - \boldsymbol{a}_l$, that is, $\boldsymbol{j} = -e^2 D(\boldsymbol{A} + \boldsymbol{a}_t)$.

By minimizing the total free energy with respect to the vector potential $\frac{\partial F}{\partial A} = \boldsymbol{0}$, we obtain the Maxwell equation $\mu_0\boldsymbol{j} = \nabla\times\boldsymbol{B}$, which in the Coulomb gauge reads

$$\nabla^2\boldsymbol{A} = e^2\mu_0 D[\boldsymbol{A} + \boldsymbol{a}_t]\delta(z). \tag{4}$$

The solution of this equation for a given distribution of the anomalous background gauge field $\boldsymbol{a}(\boldsymbol{r})$ determines the induced vector potential and the charge current. At the solution point, by substituting the Maxwell equation back into Eq. (2), we get the change of free energy due to supercurrents generated by the magnetic impurities (see Sec. 2A in SM [24]),

$$F = -\frac{1}{2}\int d^2\boldsymbol{r}\, \boldsymbol{j}\boldsymbol{a}. \tag{5}$$

Remarkably, the free energy is determined by the supercurrent in the regions in which $\boldsymbol{a}(\boldsymbol{r})$ is finite.

We now consider magnetic regions (impurities) with in-plane magnetizations $\boldsymbol{m}_i$ located at the points $\boldsymbol{r}_i$, such that the distance between the regions is much larger than the coherence length and their sizes. In this case, the distribution of the induced supercurrents almost everywhere as well as the change of the free energy become independent on the size/shape of the impurities and the corresponding anomalous vector potential in Eq. (2) can be approximated as $\boldsymbol{a}(\boldsymbol{r}) = \frac{1}{e^2D}\sum_i \Gamma_i(\boldsymbol{m}_i \times \hat{z})\delta(\boldsymbol{r}-\boldsymbol{r}_i)$. Here, we assume the size of the magnetic regions is much smaller than the Pearl length. Unlike the previous works [25–27] considering a large magnetic region, no vortices are excited around the magnet.

By solving the Maxwell-London equation (4) and inserting the supercurrent $\boldsymbol{j} = -e^2D(\boldsymbol{A}+\boldsymbol{a}_t)$ into Eq. (5) we can identify the part of the free energy responsible for the supercurrent-induced long-range magnetic interaction (see Sec. 2B in SM [24]),

$$F_I = -\frac{\Gamma^2}{4\pi e^2 D}\sum_{i\neq i}(\hat{\boldsymbol{m}}_i\cdot\nabla)(\hat{\boldsymbol{m}}_j\cdot\nabla)V(r_{ij}) = \frac{1}{2}\sum_{i\neq j}F_I^{ij}, \tag{6}$$

where $r_{ij} = |\boldsymbol{r}_i - \boldsymbol{r}_j|$ is the distance between magnetic impurities, and $V(r)$ is the dimensionless Keldysh potential,

$$V(r) = \frac{\pi}{2}\left[H_0\left(\frac{r}{r_0}\right) - Y_0\left(\frac{r}{r_0}\right)\right]. \tag{7}$$

Here, H_0 is the Struve function, Y_0 is the Bessel function of the second kind, and r_0 is the Pearl length $r_0 = 2/e^2D\mu_0$ [17], which characterizes the screening effect of the magnetic field due to $\boldsymbol{B}^2$ term in the free-energy Eq. (2).

The appearance of the Keldysh potential is quite remarkable. Usually, it describes the electrostatic potential of a point charge confined to a polarizable insulating plane [19,20]. It interpolates between the 2D ($V \sim -\ln r$) and the 3D ($V \sim 1/r$) forms of the Coulomb potential with the crossover scale given by r_0 in Eq. (7). Here, it plays a similar role by interpolating between the 2D and 3D form of the induced DDI between the impurity spins.

Working out the derivatives in the pairwise part F_I^{ij} of the interaction energy Eq. (6) we find

$$F_I^{ij} = J_\perp(r_{ij})\hat{\boldsymbol{m}}_{i\perp}\hat{\boldsymbol{m}}_{j\perp} - J_\parallel(r_{ij})\hat{\boldsymbol{m}}_{i\parallel}\hat{\boldsymbol{m}}_{j\parallel}\ , \tag{8}$$

with

$$J_\perp(r) = -\frac{\Gamma^2}{2\pi e^2 D}\frac{1}{r}\frac{dV}{dr}, \quad J_\parallel(r) = \frac{\Gamma^2}{2\pi e^2 D}\frac{d^2V}{dr^2}. \tag{9}$$

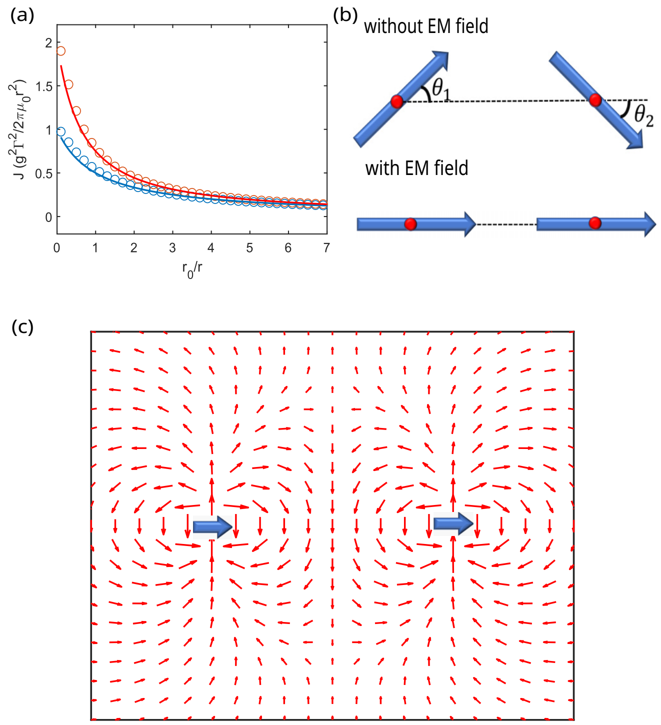

FIG. 2. (a) Superconductivity-induced magnetic interaction as a function of Pearl length. The red and blue colors denote $J_\parallel$ and $J_\perp$, respectively. The circles are the exact results calculated from Eq. (9) and the lines are the approximate values obtained from Eq. (10). (b) Ground states of two magnetic impurities with and without the EM field. (c) Distribution of the supercurrent induced by the two magnetic impurities. The distance between the two impurities is $r = r_0/2$.

To gain insight into the r dependence, it is instructive to use a highly accurate representation of $V(r)$ in terms of elementary functions [20], which yields

$$J_\perp = \frac{\Gamma^2}{2\pi e^2 D}\frac{r_0}{r^2(r+r_0)}, \quad J_\parallel = \frac{\Gamma^2}{2\pi e^2 D}\frac{r_0(2r+r_0)}{r^2(r+r_0)^2}. \tag{10}$$

The interaction as a function of the Pearl length is shown in Fig. 2(a). The important general property is that for any finite r_0, one obtains $J_\parallel > J_\perp$.

Let us analyze the case of two impurities. For convenience, we write the interaction as

$$F_I = \frac{J_\perp + J_\parallel}{2}(\hat{\boldsymbol{m}}_{1\perp}\hat{\boldsymbol{m}}_{2\perp} - \hat{\boldsymbol{m}}_{1\parallel}\hat{\boldsymbol{m}}_{2\parallel}) - \frac{J_\parallel - J_\perp}{2}\hat{\boldsymbol{m}}_1\cdot\hat{\boldsymbol{m}}_2. \tag{11}$$

The first term on the right-hand side alone does not generate a difference in the free energies of the ferromagnetic and antiferromagnetic states but rather leads to degenerate ground states with $\theta_1 = -\theta_2$, where θ_1 and θ_2 are the angles between the impurities' magnetic moments and $\boldsymbol{r}$ as shown in Fig. 2(b). The second term, with the form of an isotropic ferromagnetic interaction, breaks the ground-state degeneracy, resulting in a ferromagnetic ground state. This ferromagnetic interaction stems from the $\boldsymbol{B}^2$ term in the free energy, which was ignored in previous works [14,15]. In the limit where the EM field can be neglected $\mu_0 \to 0$ and $r_0 \to \infty$, we get $J_\parallel = J_\perp$, and in the

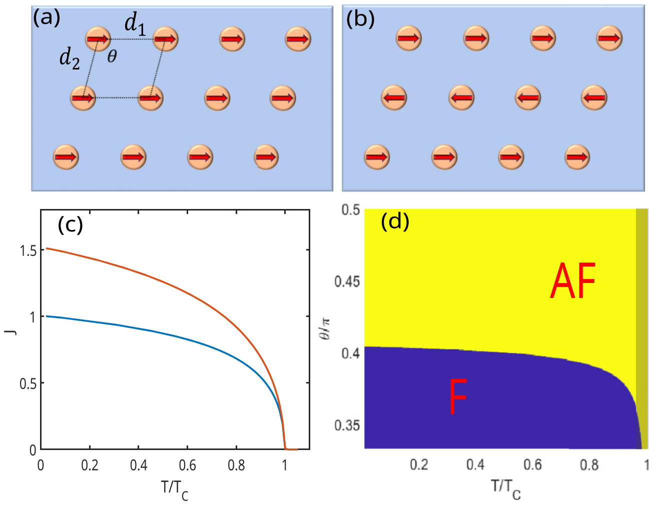

FIG. 3. (a), (b) Schematic picture of the ferromagnetic and the layered antiferromagnetic states of a Bravais magnetic impurity lattice. (c) Temperature dependence of the interaction strength. The red line and blue line denote $J_\parallel$ and $J_\perp$, respectively, in units of $J_\perp(T=0)$. The distance between the two impurities is $r = r_0(T = 0)/2$. (d) Phase diagram for a 2D impurity lattice. The lattice constant here is $d_1 = d_2 = r_0(T = 0)/50$. When T is close to T_c (gray shaded region), the Pearl length becomes too long and there might be numerical uncertainties due to the finite-size effect.

case of superconductors with large Rashba SOC we recover the result of Ref. [15] (see Sec. 3 in SM [24]).

The supercurrent $\boldsymbol{j}(\boldsymbol{r})$ induced by a magnetic impurity with magnetization $\boldsymbol{m}$ at the origin, takes the form [24]

$$\boldsymbol{j}(\boldsymbol{m},\boldsymbol{r}) = \frac{e^2D}{\Gamma}[J_\parallel \hat{\boldsymbol{m}} \times \hat{z} - (J_\parallel + J_\perp)(\hat{\boldsymbol{m}} \times \hat{z} \cdot \hat{r})\hat{r}], \tag{12}$$

where $\hat{r} \equiv \boldsymbol{r}/|\boldsymbol{r}|$. Due to the linearity of the problem, the total current induced by all impurities is given by the sum $\boldsymbol{j}_{\text{tot}} = \sum_i \boldsymbol{j}(\boldsymbol{m}_i, \boldsymbol{r} - \boldsymbol{r}_i)$. The current distribution for two impurities is shown in Fig. 2(c). Experimentally, the supercurrent distribution can be determined by measuring the local current-induced magnetic field [28].

Superconductivity-induced ferromagnetism in a 2D Bravais lattice. Next, we consider an infinite Bravais lattice of magnetic impurities, as shown in Fig. 3(a). Below we assume $d_1 = d_2$ and the shape of the lattice is controlled by the angle θ. It is a triangular lattice when $\theta = \pi/3$ and a square lattice when $\theta = \pi/2$. Here, we concentrate on the case where θ is between $\pi/3$ and $\pi/2$. In this system, the interaction energy density is given by $E = \frac{1}{2V}\sum_{i\neq j} F_I^{ij}$, where V is the area of the 2D lattice. We notice that the inclusion of the EM field is crucial for computing energy. Otherwise, the interaction F_I^{ij} scales as $1/r^2$ and the energy density unphysically diverges in the thermodynamics limit. With the screening effect of the EM field, according to Eq. (10), F_I^{ij} crosses over from the 2D to 3D DDI and decays as $1/r^3$ at $r \to \infty$, resulting in convergent and extensive energy.

The 3D DDI-induced ordered state in a 2D electric dipole lattice has been studied in Ref. [29]. It has been shown that a ferroelectric state forms in a triangular lattice, while a square lattice favors a layered antiferroelectric state. Since the superconductivity-induced magnetic interaction has a form between 2D and 3D DDI, we expect similar ground states in our model. By minimizing the energy we find that at $T = 0$ the ground state can be either a ferromagnetic state [Fig. 3(a)] induced by the net ferromagnetic interaction $\frac{J_\parallel - J_\perp}{2}$, or a layered antiferromagnetic state [Fig. 3(b)] due to the 2D DDI $\frac{J_\parallel + J_\perp}{2}$. At finite temperatures, the order parameter $\Delta(T)$ needs to be determined self-consistently. The superfluid weight D and the Pearl length r_0 are calculated using $\Delta(T)$. The corresponding temperature dependence of $J_\parallel$ and $J_\perp$ is shown in Fig. 3(c). With increasing temperature, the superfluid weight is decreased, leading to the suppression of the magnetic interaction. In addition, the relative value of the net ferromagnetic interaction $\frac{J_\parallel - J_\perp}{2}$ compared with the 2D DDI $\frac{J_\parallel + J_\perp}{2}$ becomes smaller at higher temperatures, suggesting a transition to an antiferromagnetic phase at some finite temperature. The phase diagram obtained numerically is shown in Fig. 3(d). At $T = 0$, the triangular lattice ($\theta = \pi/3$) has a ferromagnetic ground state, while the square lattice is antiferromagnetic. By setting $\mu_0 \to 0$, we find that the ground state is always an antiferromagnetic state without the magnetic field.

Example: Iron-based superconductor. Recent experiments [21,30–33], provide compelling evidence of observing a ferromagnetic ordering in the superconducting state. Specifically, in Ref. [21], a hysteretic magnetization was observed in Fe(Se,Te) with Fe impurities only when the system is in the superconducting state. This observation suggests that it may be the supercurrent that mediates the interaction between the magnetic impurities. According to Refs. [30,33], the ferromagnetism dwells on the surface of the superconductor, indicating that the SOC is crucial for the formation of the ferromagnetic state. It is also believed that the topological surface band is of Dirac type [34,35] and therefore it can be described by the Hamiltonian

$$H_0 = (-iv\nabla \times \boldsymbol{\sigma} - \mu)\tau_3 + \Delta\tau_1 + \sum_i \mathcal{J}_0 \boldsymbol{m}_i \cdot \boldsymbol{\sigma}\delta(\boldsymbol{r} - \boldsymbol{r}_i),$$

where v is the Fermi velocity, μ is the chemical potential, $\mathcal{J}_0$ is the exchange interaction, and the last term describes the exchange field induced by magnetic impurities. The anomalous currents induced locally at the impurities and entering our theory via the parameter Γ can be expressed straightforwardly in terms of the impurity scattering T matrix (see Sec. 4 in SM [24]). Realistic values of effective parameters for Fe(Se,Te) are given by [36,37] $v = 0.216$ eV Å, $E_F = 4.5$ meV, $\Delta = 1.5$ meV, $|\boldsymbol{m}| = 5$, $\mathcal{J}_0 = 50\text{ meV} \times (0.4\text{ nm})^2$. With these values, we obtain that at $T = 0$ the supercurrent-mediated magnetic interaction between two magnetic impurities separated by 10 nm is of the order of meV, comparable with the superconducting gap. Thus, thermal fluctuations can be neglected for low enough temperatures $T \ll \Delta$.

Conclusion. We have demonstrated that a combination of London-Pearl screening and magnetoelectric effects can induce long-range magnetic interactions between impurities in superconductors. We have shown that the induced magnetic interaction has the form of a 2D dipole-dipole interaction combined with a ferromagnetic coupling. In addition to possible candidates such as the discussed iron-based superconductors or 2D superconducting structures with a polar axis perpendicular to the plane, our results should be valid for any superconductor showing a magnetoelectric effect. These are gyrotropic superconductors as discussed in Ref. [38]. Examples of these are Li_2Pt_3B, Li_2Pd_3, B [39,40], Mo_3Al_2C [41], $TaRh_2B_2$, $NbRh_2B_2$ [42], and T_d-WTe_2 [43,44]. Also interesting are materials with isotropic gaps exhibiting intrinsic magnetism (see Ref. [45] and references therein). Among these materials, $LaNiC_2$, $La_7(Ir, Rh)_3$, and Zr_3Ir are gyrotropic and hence they may exhibit the magnetoelectric effect. Our predicted effect may be relevant for explaining the intrinsic magnetism observed in these materials.

Finally, applications of our effect in superconducting spintronics [46,47] are envisioned, where low-dissipation electric currents can be used to spin-polarize systems.

Acknowledgments. We acknowledge financial support from Spanish AEI (MCIN/AEI/10.13039/501100011033) through projects PID2020-114252GB-I00 (SPIRIT), TED2021-130292B-C42, and PID2020-112811GB-I00. We also acknowledge the Basque Government support through the program Grupos Consolidados, grants IT-1591-22 and IT1453-22, and through the IKUR strategy program.

[1] P. W. Anderson and H. Suhl, Phys. Rev. **116**, 898 (1959).
[2] A. I. Buzdin, Rev. Mod. Phys. **77**, 935 (2005).
[3] F. S. Bergeret, A. F. Volkov, and K. B. Efetov, Rev. Mod. Phys. **77**, 1321 (2005).
[4] F. S. Bergeret, A. F. Volkov, and K. B. Efetov, Phys. Rev. B **69**, 174504 (2004).
[5] J. Xia, V. Shelukhin, M. Karpovski, A. Kapitulnik, and A. Palevski, Phys. Rev. Lett. **102**, 087004 (2009).
[6] F. S. Bergeret, A. F. Volkov, and K. B. Efetov, Europhys. Lett. **66**, 111 (2004).
[7] P. G. De Gennes, Phys. Lett. **23**, 10 (1966).
[8] L. R. Tagirov, Phys. Rev. Lett. **83**, 2058 (1999).
[9] Y. A. Izyumov, Y. N. Proshin, and M. G. Khusainov, Phys. Usp. **45**, 109 (2002).
[10] R. Ojajärvi, F. S. Bergeret, M. A. Silaev, and T. T. Heikkilä, Phys. Rev. Lett. **128**, 167701 (2022).
[11] V. M. Edelstein, Phys. Rev. Lett. **75**, 2004 (1995).
[12] F. Konschelle, I. V. Tokatly, and F. S. Bergeret, Phys. Rev. B **92**, 125443 (2015).
[13] F. S. Bergeret and I. V. Tokatly, Phys. Rev. B **102**, 060506(R) (2020).
[14] S. S. Pershoguba, K. Björnson, A. M. Black-Schaffer, and A. V. Balatsky, Phys. Rev. Lett. **115**, 116602 (2015).
[15] A. G. Mal'shukov, Phys. Rev. B **98**, 054504 (2018).
[16] The ferromagnetic ordering has been considered in Ref. [15] by neglecting the screening effects. This approach resulted in an unphysical dependence on sample geometry, making the results inconclusive in the thermodynamic limit. Additionally, the study did not explore the potential existence of competing phases.
[17] J. Pearl, Appl. Phys. Lett. **5**, 65 (1964).
[18] It is important to emphasize that we focus on superconductors with magnetic impurities, with the ferromagnetic coupling stemming solely from the interplay between the superfluidity and the magnetoelectric effect. In this regard, our work differs from other studies that concentrate on hypothetical intrinsic magnetic states in superconductors with time-reversal symmetry breaking without magnetic impurities [45,48–50].
[19] L. V. Keldysh, Pis'ma Zh. Eksp. Teor. Fiz. **29**, 716 (1979) [JETP Lett. **29**, 658 (1979)].
[20] P. Cudazzo, I. V. Tokatly, and A. Rubio, Phys. Rev. B **84**, 085406 (2011).
[21] B. K. Xiang, Y. S. Lin, Q. S. He, J. J. Zhu, B. R. Chen, Y. F. Wang, K. Y. Liang, Z. J. Li, H. X. Yao, C. X. Wu *et al.*, arXiv:2307.10722.
[22] F. S. Bergeret and I. V. Tokatly, Europhys. Lett. **110**, 57005 (2015).
[23] E. Strambini, A. Iorio, O. Durante, R. Citro, C. Sanz-Fernández, C. Guarcello, I. V. Tokatly, A. Braggio, M. Rocci, N. Ligato *et al.*, Nat. Nanotechnol. **15**, 656 (2020).
[24] See Supplemental Material at http://link.aps.org/supplemental/10.1103/PhysRevB.108.L180506 for the derivations of Γ parameters in different systems, the derivations of the superconductivity-induced magnetic interaction, comparison with the previous work, and a microscopic analysis of Fe(Se,Te), which includes Refs. [51,52].
[25] A. V. Samokhvalov, J. Exp. Theor. Phys. **135**, 897 (2022).
[26] L. A. B. Olde Olthof, X. Montiel, J. W. A. Robinson, and A. I. Buzdin, Phys. Rev. B **100**, 220505(R) (2019).
[27] A. G. Mal'shukov, Phys. Rev. B **102**, 144503 (2020).
[28] Y. S. Lin, S. Y. Wang, X. Zhang, Y. Feng, Y. P. Pan, H. Ru, J. J. Zhu, B. K. Xiang, K. Liu, C. L. Zheng *et al.*, Phys. Rev. X **13**, 011046 (2023).
[29] V. Rozenbaum, Zh. Eksp. Teor. Fiz. **99**, 1836 (1991).
[30] G. Qiu, H.-Y. Yang, L. Hu, H. Zhang, C.-Y. Chen, Y. Lyu, C. Eckberg, P. Deng, S. Krylyuk, A. V. Davydov *et al.*, arXiv:2303.00966.
[31] N. Zaki, G. Gu, A. Tsvelik, C. Wu, and P. D. Johnson, Proc. Natl. Acad. Sci. USA **118**, e2007241118 (2021).
[32] N. J. McLaughlin, H. Wang, M. Huang, E. Lee-Wong, L. Hu, H. Lu, G. Q. Yan, G. Gu, C. Wu, Y.-Z. You *et al.*, Nano Lett. **21**, 7277 (2021).
[33] C. Farhang, N. Zaki, J. Wang, G. Gu, P. D. Johnson, and J. Xia, Phys. Rev. Lett. **130**, 046702 (2023).
[34] Z. Wang, P. Zhang, G. Xu, L. K. Zeng, H. Miao, X. Xu, T. Qian, H. Weng, P. Richard, A. V. Fedorov, H. Ding, X. Dai, and Z. Fang, Phys. Rev. B **92**, 115119 (2015).
[35] X. Wu, S. Qin, Y. Liang, H. Fan, and J. Hu, Phys. Rev. B **93**, 115129 (2016).
[36] K. Jiang, X. Dai, and Z. Wang, Phys. Rev. X **9**, 011033 (2019).
[37] V. Thampy, J. Kang, J. A. Rodriguez-Rivera, W. Bao, A. T. Savici, J. Hu, T. J. Liu, B. Qian, D. Fobes, Z. Q. Mao, C. B. Fu, W. C. Chen, Q. Ye, R. W. Erwin, T. R. Gentile, Z. Tesanovic, and C. Broholm, Phys. Rev. Lett. **108**, 107002 (2012).
[38] W.-Y. He and K. T. Law, Phys. Rev. Res. **2**, 012073(R) (2020).
[39] H. Q. Yuan, D. F. Agterberg, N. Hayashi, P. Badica, D. Vandervelde, K. Togano, M. Sigrist, and M. B. Salamon, Phys. Rev. Lett. **97**, 017006 (2006).
[40] K. Togano, P. Badica, Y. Nakamori, S. Orimo, H. Takeya, and K. Hirata, Phys. Rev. Lett. **93**, 247004 (2004).

[41] A. B. Karki, Y. M. Xiong, I. Vekhter, D. Browne, P. W. Adams, D. P. Young, K. R. Thomas, J. Y. Chan, H. Kim, and R. Prozorov, Phys. Rev. B **82**, 064512 (2010).

[42] E. M. Carnicom, W. Xie, T. Klimczuk, J. Lin, K. Górnicka, Z. Sobczak, N. P. Ong, and R. J. Cava, Sci. Adv. **4**, eaar7969 (2018).

[43] J.-K. Kim, K.-R. Jeon, P. K. Sivakumar, J. Jeon, C. Koerner, G. Woltersdorf, and S. S. P. Parkin, arXiv:2303.13049.

[44] In this Letter, we focus on two-dimensional materials with a polar vector perpendicular to the transport plane. Other gyrotropic superconductors may be three-dimensional materials. The relation between the anomalous current $\mathbf{j}_{\mathrm{an}}$ and the effective potential $\mathbf{a}$ depends on the specific symmetry [38].

[45] S. K. Ghosh, M. Smidman, T. Shang, J. F. Annett, A. D. Hillier, J. Quintanilla, and H. Yuan, J. Phys.: Condens. Matter **33**, 033001 (2021).

[46] M. Eschrig, Phys. Today **64**(1), 43 (2011).

[47] J. Linder and J. W. A. Robinson, Nat. Phys. **11**, 307 (2015).

[48] A. Ramires, J. Phys.: Condens. Matter **34**, 304001 (2022).

[49] C. N. Breiø, P. J. Hirschfeld, and B. M. Andersen, Phys. Rev. B **105**, 014504 (2022).

[50] G. Csire, J. F. Annett, J. Quintanilla, and B. Újfalussy, Phys. Rev. B **106**, L020501 (2022).

[51] A. V. Balatsky, I. Vekhter, and J.-X. Zhu, Rev. Mod. Phys. **78**, 373 (2006).

[52] M. Houzet and J. S. Meyer, Phys. Rev. B **92**, 014509 (2015).